Journal of Mathematical Sciences
https://doi.org/10.1007/s10958-025-07602-w

# MODELING THE RAILWAY TRACK BALLAST BEHAVIOR WITH HYPOPLASTICITY

**Erich Bauer[1] · Victor A. Kovtunenko[2,3] · Pavel Krejčí[4] · Giselle A. Monteiro[5] · Laetitia Paoli[6] · Adrien Petrov[7]**

Accepted: 29 January 2025


**Abstract**

The contact problem describing a railway vehicle — road — track ballast system is under our investigation. During the motion, the rolling stock (snowpiercer) is represented by a moving localized load, the road by a Timoshenko beam, and the track bed material is rigorously modeled using 3-by-3 matrices of stress and strain rate. To ensure physical consistency, the Kolymbas-type hypoplasticity theory well-suited for cohesionless granular materials is applied to describe the ballast. As a result, the normal stress and shear stress on the interface between the rail bottom and ballast are analytically derived from the closed-form solution to the nonlinear hypoplastic differential equation.

**Keywords** Contact and vehicle dynamic · Railway modeling · Track ballast material · Hypoplasticity

All authors contributed equally to this work.

✉ Victor A. Kovtunenko
victor.kovtunenko@uni-graz.at

Erich Bauer
erich.bauer@tugraz.at

Pavel Krejčí
krejci@math.cas.cz

Giselle A. Monteiro
gam@math.cas.cz

Laetitia Paoli
laetitia.paoli@univ-st-etienne.fr

Adrien Petrov
apetrov@math.univ-lyon1.fr

1 Graz University of Technology, Technikerstr. 4, Graz 8010, Austria

2 Department of Mathematics and Scientific Computing, Karl-Franzens University of Graz, NAWI Graz, Heinrichstr. 36, Graz 8010, Austria

3 Lavrentyev Institute of Hydrodynamics, Siberian Division of the Russian Academy of Sciences, Novosibirsk 630090, Russia

4 Faculty of Civil Engineering, Czech Technical University in Prague, Thákurova 7, Praha 6 166 29, Czech Republic

5 Institute of Mathematics, Czech Academy of Sciences, Žitná 25, Praha 1 115 67, Czech Republic

6 Université Jean Monnet, CNRS, Ecole Centrale de Lyon, INSA Lyon, Universite Claude Bernard Lyon 1, ICJ UMR5208, 42023 Saint-Etienne, France

7 INSA Lyon, CNRS, Ecole Centrale de Lyon, Universite Claude Bernard Lyon 1, Université Jean Monnet, ICJ UMR5208, 20 Avenue A. Einstein, Villeurbanne 69621, France

Published online: 22 February 2025

## Introduction

Trains traveling over railway tracks create a complex, multi-scale, and multi-physics system for dynamic contact. During rolling contact, high contact stress, temperature fluctuations, elasto-plastic deformation, and friction forces may cause wear phenomena on the rails, such as cracks, material wear, and the generation of wear debris between the contacting surfaces. These phenomena are also accompanied by chemical reactions and squeal noise effects.

By neglecting these complex phenomena, many mathematical models consider the rails as Euler-Bernouilli beams subjected to a moving load from rolling stock and supported by rigid foundations [1], or constrained between two rigid obstacles [2, 3]. An elastic foundation composed of continuously distributed linear elastic springs together with Coulomb frictional dampers was modeled and analyzed in [4]. The mechanical properties of a viscoelastic spring foundation were expressed using both frictional and viscous dampers in [5]. These mathematical problems are non-smooth and are governed by partial differential inclusions.

A railway track is composed of several key components, including rails, fasteners, sleepers, and a track bed known as ballast, which lies between the natural ground. The track ballast supports the static load of the rails as well as the dynamic load from rolling stock, and also aids in drainage. It is typically composed of aggregate grains made from crushed stones, gravel, sand, and their mixtures. A recent survey on the development of railway track technologies can be found in [6]. The survey highlights that the ballast is the weakest element of the track, heavily influenced by the material used in the bed. As trains pass over the track, the angularity of the ballast grains diminishes, producing fine particles and leading to irreversible deformation of the ballast structure and consequently to a decline in track performance. Some micro-Deval abrasion tests and discrete element simulations of ballast wear have been conducted in [7]. Therefore, accurately accounting for ballast behavior might be the primary challenge in modeling a snowpiercer.

In the present paper, we use the Timoshenko beam equation instead of the Euler-Bernoulli beam equation to model the rail, in order to take into account more accurately the shear effects in the cross-section of the beam (see [8–11]). For papers dealing with the coupling of the Timoshenko beam with the elastic medium, we cite [12–14]. Moreover, the track ballast with dissipative material properties is rigorously modeled using 3-by-3 stress and strain rate matrices within the framework of hypoplastic theory, as developed by Kolymbas and co-authors [15–17] to describe cohesionless granular materials. Specifically, we employ a simplified version of the hypoplastic constitutive model introduced by Bauer [18] and Gudehus [19]. In previous studies, the hypoplastic strain-stress response as a nonlinear differential equation is established. In [20, 21], a solution for the stress under a prescribed proportional strain rate, called strain control, was derived in the closed-form. Conversely, an unknown strain rate entering implicit differential equations under a given proportional stress, called stress control, was obtained analytically in [22].

In the "The railway vehicle-road model" section, we present a physical model of frictional contact, activated by a localized force moving at a given velocity over the Timoshenko beam. We assume the beam to be linear elastic, isotropic, and homogeneous, with a constant cross-section. This beam lies on a deformable track ballast occupying a semi-infinite strip of constant height, modeled as a hypoplastic granular material in a simplified manner. In order to preserve the continuity of displacement of the ballast layer, a distribution of the vertical displacement field and rotation field linear decreasing with the depth is introduced. The closed-form solution to the nonlinear hypoplastic differential equation, the normal stress and shear stress acting on the bottom of the beam are provided analytically in the "The hypoplastic ballast model" section.

## The railway vehicle-road model

We consider the dynamic contact problem for the railway vehicle-road model as illustrated in $(x, y, z)$-coordinate system at some fixed time $t$ [s] in Fig. 1. For simplicity, the whole problem is assumed to be under plane strain conditions, i.e., there is no deformation in the direction of the $y$-coordinate. The rail vehicle (snowpiercer) is represented by a localized vertical load $\mathbf{F}$ moving at a velocity $V(t)$ [m/s] in contact with the railroad along the $x$-direction.

We model the railroad as a Timoshenko beam with a height $h_\mathrm{b}$ and constant mass density $\varrho$ [kg/m$^3$], cross-section area A [m$^2$], second moment of area I [m$^4$], Timoshenko shear coefficient $\kappa$ [1] which depends on the geometry and $\mathbb{E}$ [N/m$^2$] and $\mathbb{S}$ [N/m$^2$] are the elastic and shear modulus, respectively. For convenience, we assume the $x$-axis to be the center-line of the undeformed beam in the reference configuration fulfilling the condition $\int_{-h_\mathrm{b}/2}^{h_\mathrm{b}/2} \xi \, dA = 0$. Herein $\xi$ denotes the local

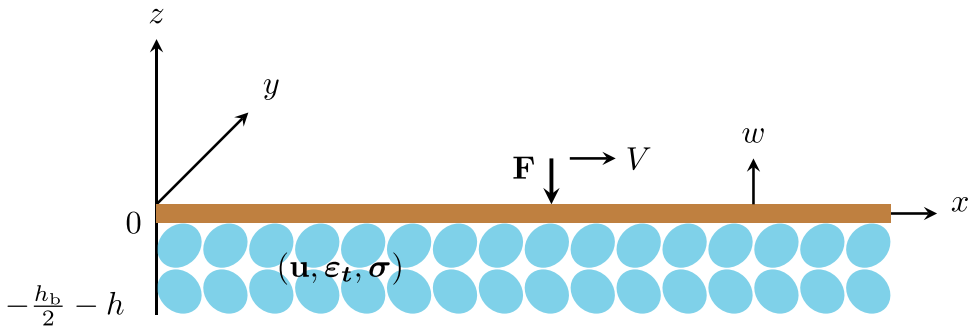


**Fig. 1** Geometry of the railway vehicle-road model

coordinate in the cross-section measured from the $(x, y)$-plane located at half height of the beam. In Timoshenko beam theory the displacements of the beam are assumed to be given by $\mathbf{v}(t,x,\xi) \overset{\text{def}}{=} (v_1, v_2, v_3)$ with

$$v_1(t,x,\xi) = u_c(t,x) - \xi\theta(t,x), \quad v_2(t,x,\xi) = 0, \quad v_3(t,x,\xi) = w(t,x).$$

Here, $w(t, x)$ [m] denotes the vertical deflection of the center-line of the beam, $u_c(t,x)$ [m] stands for the longitudinal displacement of the center-line, while $\theta(t,x)$ [rad] is the rotation angle of the cross-section of the beam with respect to the vertical direction.

In its turn, the railroad represents the contact boundary with a track ballast of height $h$ lying in the half-space $z < -h_b/2$ and described by the displacement vector $\mathbf{u}(t,x,z)$ [m], strain rate $\boldsymbol{\varepsilon}_t(t,x,z)$ [1/s] and stress state $\boldsymbol{\sigma}(t,x,z)$ [N/m$^2$] tensors. By using the above notations, the Timoshenko beam can be described by the following three equations of motion stated at the center-line corresponding to $z = 0$:

$$\begin{cases} \varrho\,\mathrm{A}\,u_{ctt}(t,x) = \dfrac{\partial}{\partial x}\Big(\mathbb{E}\,\mathrm{A}\,u_{cx}(t,x)\Big) - \ell\,\sigma_{31}(t,x), & \text{(1a)} \\ \varrho\,\mathrm{A}\,w_{tt}(t,x) = \dfrac{\partial}{\partial x}\Big(\kappa\,\mathrm{A}\,\mathbb{S}\big[w_x(t,x) - \theta(t,x)\big]\Big) - \varrho\mathrm{A}g + q(t,x) - \ell\,\sigma_{33}(t,x), & \text{(1b)} \\ \varrho\,\mathrm{I}\,\theta_{tt}(t,x) = \dfrac{\partial}{\partial x}\Big(\mathbb{E}\,\mathrm{I}\,\theta_x(t,x)\Big) + \kappa\,\mathrm{A}\,\mathbb{S}\big[w_x(t,x) - \theta(t,x)\big] - \dfrac{h_b}{2}\,\ell\,\sigma_{31}(t,x), & \text{(1c)} \end{cases}$$

for all $(t,x) \in (t_0, T) \times \mathbb{R}$ with $T > t_0$. We denote by $(\cdot)_t \overset{\text{def}}{=} \frac{\partial}{\partial t}$ and $(\cdot)_x \overset{\text{def}}{=} \frac{\partial}{\partial x}$ the derivatives with respect to $t$ and $x$, respectively. In the vertical direction, $\varrho\mathrm{A}g$ accounts for the weight of the beam per unit length in which $g$ [m/s$^2$] denotes the gravitational acceleration. In equation (1b), the quantity

$$q \overset{\text{def}}{=} -\mathbf{F}\psi(x - X(t))$$

defines the applied moving load, $\psi : \mathbb{R} \to [0,1]$ is an even, $\mathrm{C}^2$-class function such that $\mathrm{supp}\psi \subset [-\delta, \delta]$ and $\int_{\mathbb{R}} \psi(x)\mathrm{d}x = 1$, with $\delta > 0$ that represents a finite-scale vehicle-rail contact area, $X(t) \overset{\text{def}}{=} \int_{t_0}^{t} V(s)\mathrm{d}s$. Parameter $\ell$ [m] denotes a characteristic length.

We prescribe initial data $\mathbf{v}(t_0,\cdot) = \mathbf{v}^0$ and $\mathbf{v}_t(t_0,\cdot) = \mathbf{v}_t^0$. From an engineering viewpoint, the initial rotation angle $\theta(t_0,\cdot) = \theta^0$ and $\theta_t(t_0,\cdot) = \theta_t^0$ can be obtained from the initial location of load $\mathbf{F}\psi(x - X(t_0))$. The reaction of ballast to rail implies normal stresses $\mathbf{n}\cdot\boldsymbol{\sigma}(t,x)\mathbf{n} = \sigma_{33}(t,x)$ with the outward normal vectors $\mathbf{n} = (0,0,1)$ and shear stresses $\sigma_{13}(t,x)$ on the boundary $z = -h_b/2$. Equation (1a) describes the effect of the interface shear stress $\sigma_{13}(t,x)$ on the longitudinal displacement $u_c(t,x)$ of the center-line of the beam. Combining (1b) with (1c) leads to a fourth-order differential equation for the unknown $w(t,x)$.

For a frictional contact between the rail and the ballast, we assume that the top of the ballast follows the deformed bottom profile of the beam. Consideration of the undeformed top surface of the ballast at $z = -h_b/2$ as reference level the displacement vector of the interface has the following components:

$$\mathbf{u}_{\mathrm{BT}} = \Big[u_c(t,x) + \frac{h_b}{2}\,\theta(t,x),\ 0\,,\ w(t,x)\Big]. \tag{2}$$

In the half-space $z < -h_\mathrm{b}/2$, the ballast is assumed to occupy a semi-infinite strip of height $h$ [m] which is fixed at the bottom:

$$\mathbf{u} = (0,0,0) \quad \text{at} \quad z = -\frac{h_\mathrm{b}}{2} - h. \tag{3}$$

In order to fit the both boundary conditions (2) and (3), we propose a linear distribution of the displacement across the $z$-variable in the ballast such that for $z \in [-h_\mathrm{b}/2 - h, -h_b/2]$:

$$\mathbf{u}(t,x,z) \overset{\text{def}}{=} \left[\frac{2\,u_c + h_\mathrm{b}\,\theta}{4\,h}\,\big(h_\mathrm{b} + 2\,h + 2\,z\big),\, 0\,,\, \frac{w}{2\,h}\big(h_\mathrm{b} + 2\,h + 2\,z\big)\right]. \tag{4}$$

In the next section, we specify material model for the ballast satisfying (4) and express explicitly the normal stress $\sigma_{33}(t,x)$ and shear stress $\sigma_{13}(t,x)$ in the balance equations (1a), (1b), and (1c).

## The hypoplastic ballast model

A typical track bed is composed of grains like rock, gravel, sand, and their mixture. Thus, we employ a hypoplastic model, which is well-suited for describing cohesionless granular materials. Let us introduce the orthogonal decomposition into deviatoric and spherical components with the identity tensor $\mathbf{I}$:

$$\boldsymbol{\sigma} \overset{\text{def}}{=} \boldsymbol{\sigma}^\star + \frac{1}{3}\mathrm{tr}(\boldsymbol{\sigma})\mathbf{I}.$$

We consider the constitutive response between the stress $\boldsymbol{\sigma}$, stress rate $\boldsymbol{\sigma}_t$ [N/(m$^2$s)] and strain rate $\boldsymbol{\varepsilon}_t$ [1/s] as given by (see [18, 20, 22]):

$$\boldsymbol{\sigma}_t = f_\mathrm{s}\Big(a^2\mathrm{tr}(\boldsymbol{\sigma})\boldsymbol{\varepsilon}_t + \frac{\boldsymbol{\sigma} : \boldsymbol{\varepsilon}_t}{\mathrm{tr}(\boldsymbol{\sigma})}\boldsymbol{\sigma} + a f_\mathrm{d}(\boldsymbol{\sigma} + \boldsymbol{\sigma}^\star)\|\boldsymbol{\varepsilon}_t\|\Big), \tag{5}$$

where $\|\boldsymbol{\varepsilon}_t\|$ stands for the Frobenius norm, $a > 0$ denotes a constant yield strength, $f_\mathrm{s} < 0$ and $f_\mathrm{d} > 0$ are the stiffness and density factors. These factors may be inhomogeneous when depending on void ratio [23], in this work, however, we neglect the influence of the void ratio, and the factors $f_s$ and $f_d$ are assumed to be constants. As a consequence of equations (7a)–(7c) below, the components of the strain rate tensor $\boldsymbol{\varepsilon}_t$ in the hypoplastic constitutive equation (5) are functions of the time derivatives of $u_c$, $\theta$, $\theta_x$, $w$, $w_x$.

By differentiating (4), we calculate the strain rate components $\varepsilon_{ijt} \overset{\text{def}}{=} \frac{1}{2}\big(\frac{\partial u_{it}}{\partial x_j} + \frac{\partial u_{jt}}{\partial x_i}\big)$, $i,j = 1,2,3$, as follows:

$$\boldsymbol{\varepsilon}_t \overset{\text{def}}{=} \begin{pmatrix} \varepsilon_{11t} & 0 & \varepsilon_{13t} \\ 0 & 0 & 0 \\ \varepsilon_{31t} & 0 & \varepsilon_{33t} \end{pmatrix}, \tag{6}$$

where

$$\begin{cases} \varepsilon_{11t} \overset{\text{def}}{=} \dfrac{2\,u_{ctx} + h_\mathrm{b}\,\theta_{tx}}{4\,h}\,\big(h_\mathrm{b} + 2\,h + 2\,z\big), & \text{(7a)} \\ \varepsilon_{13t} = \varepsilon_{31t} \overset{\text{def}}{=} \dfrac{1}{4\,h}\Big(2\,u_{ct} + h_\mathrm{b}\,\theta_t + w_{tx}\big(h_\mathrm{b} + 2\,h + 2\,z\big)\Big), & \text{(7b)} \\ \varepsilon_{33t} \overset{\text{def}}{=} \dfrac{1}{h}w_t. & \text{(7c)} \end{cases}$$

Rescaling the stress, let us consider

$$\hat{\boldsymbol{\sigma}} \overset{\text{def}}{=} \frac{\boldsymbol{\sigma}}{\text{tr}(\boldsymbol{\sigma})} = \hat{\boldsymbol{\sigma}}^{\star} + \frac{1}{3}\mathbf{I}. \tag{8}$$

Note that the decomposition into deviatoric and spherical parts yields

$$\hat{\boldsymbol{\sigma}}_t^{\star} = \hat{\boldsymbol{\sigma}}_t = \frac{\boldsymbol{\sigma}_t}{\text{tr}(\boldsymbol{\sigma})} - \frac{\hat{\boldsymbol{\sigma}}}{\text{tr}(\boldsymbol{\sigma})}\text{tr}(\boldsymbol{\sigma}_t), \tag{9}$$

while from (5), we deduce that

$$\text{tr}(\boldsymbol{\sigma}_t) = f_{\text{s}}\big(a^2\text{tr}(\boldsymbol{\sigma})\text{tr}(\boldsymbol{\varepsilon}_t) + \boldsymbol{\sigma} : \boldsymbol{\varepsilon}_t + af_{\text{d}}\text{tr}(\boldsymbol{\sigma})\|\boldsymbol{\varepsilon}_t\|\big). \tag{10}$$

Therefore, the constitutive response (5) can be decomposed equivalently with respect to normalized stress:

$$\hat{\boldsymbol{\sigma}}_t^{\star} = f_{\text{s}}a\big(a\boldsymbol{\varepsilon}_t - a\text{tr}(\boldsymbol{\varepsilon}_t)\hat{\boldsymbol{\sigma}} + f_{\text{d}}\|\boldsymbol{\varepsilon}_t\|\hat{\boldsymbol{\sigma}}^{\star}\big). \tag{11}$$

Using the identities in (8), we can see that

$$\boldsymbol{\sigma} : \boldsymbol{\varepsilon}_t = \text{tr}(\boldsymbol{\sigma})\left(\hat{\boldsymbol{\sigma}}^{\star} : \boldsymbol{\varepsilon}_t + \frac{\text{tr}(\boldsymbol{\varepsilon}_t)}{3}\right),$$

therefore, rewriting (10)–(11), we obtain the following 1st-order ODE system with respect to stress:

$$\hat{\boldsymbol{\sigma}}_t^{\star} = f_{\text{s}}a\left(a\left(\boldsymbol{\varepsilon}_t - \frac{\text{tr}(\boldsymbol{\varepsilon}_t)}{3}\mathbf{I}\right) + \big(f_{\text{d}}\|\boldsymbol{\varepsilon}_t\| - a\text{tr}(\boldsymbol{\varepsilon}_t)\big)\hat{\boldsymbol{\sigma}}^{\star}\right), \tag{12a}$$

$$\text{tr}(\boldsymbol{\sigma}_t) = f_{\text{s}}\left(\left(a^2 + \frac{1}{3}\right)\text{tr}(\boldsymbol{\varepsilon}_t) + \hat{\boldsymbol{\sigma}}^{\star} : \boldsymbol{\varepsilon}_t + af_{\text{d}}\|\boldsymbol{\varepsilon}_t\|\right)\text{tr}(\boldsymbol{\sigma}), \tag{12b}$$

endowed with initial conditions

$$\boldsymbol{\sigma} = \boldsymbol{\sigma}^0 \quad \text{at} \quad t = t_0. \tag{13}$$

We will solve the coupled system of linear equations in closed form.

**Theorem 1** (Analytical solution) *Under the strain control* (6)*, there exists an analytical solution to the Cauchy problem* ()–(13) *expressed in the closed-form, where we write only the dependency on t to simplify the notation*:

$$\bullet\ \hat{\sigma}_{ij}^{\star}(t) = \hat{\sigma}_{ij}^{\star}(t_0)\text{E}(\boldsymbol{\varepsilon}(t)) \quad \text{for} \quad ij = 12, 23, \tag{14a}$$

$$\bullet\ \hat{\sigma}_{13}^{\star}(t) = c_{13}(t)\text{E}(\boldsymbol{\varepsilon}(t)) \quad \text{with} \quad c_{13}(t) \overset{\text{def}}{=} \hat{\sigma}_{13}^{\star}(t_0) + f_{\text{s}}a^2\int_{t_0}^{t}\frac{\varepsilon_{13t}(s)}{\text{E}(\boldsymbol{\varepsilon}(s))}\text{d}s, \tag{14b}$$

$$\bullet\ \hat{\sigma}_{22}^{\star}(t) = c_{22}(t)\text{E}(\boldsymbol{\varepsilon}(t)) \quad \text{with} \quad c_{22}(t) \overset{\text{def}}{=} \hat{\sigma}_{22}^{\star}(t_0) - \frac{f_{\text{s}}a^2}{3}\int_{t_0}^{t}\frac{\varepsilon_{11t}(s) + \varepsilon_{33t}(s)}{\text{E}(\boldsymbol{\varepsilon}(s))}\text{d}s, \tag{14c}$$

$$\bullet\ \hat{\sigma}_{11}^{\star}(t) = c_{11}(t)\text{E}(\boldsymbol{\varepsilon}(t)) \quad \text{with} \quad c_{11}(t) \overset{\text{def}}{=} \hat{\sigma}_{11}^{\star}(t_0) + \frac{f_{\text{s}}a^2}{3}\int_{t_0}^{t}\frac{2\varepsilon_{11t}(s) - \varepsilon_{33t}(s)}{\text{E}(\boldsymbol{\varepsilon}(s))}\text{d}s, \tag{14d}$$

$$\bullet\ \hat{\sigma}_{33}^{\star}(t) = c_{33}(t)\text{E}(\boldsymbol{\varepsilon}(t)) \quad \text{with} \quad c_{33}(t) \overset{\text{def}}{=} \hat{\sigma}_{33}^{\star}(t_0) + \frac{f_{\text{s}}a^2}{3}\int_{t_0}^{t}\frac{2\varepsilon_{33t}(s) - \varepsilon_{11t}(s)}{\text{E}(\boldsymbol{\varepsilon}(s))}\text{d}s, \tag{14e}$$

*recalling that* $\hat{\sigma}^{\star}_{ij}(t) = \hat{\sigma}^{\star}_{ji}(t)$, *and defining*

$$\mathrm{E}(\boldsymbol{\varepsilon}(t)) \overset{\text{def}}{=} \exp\left(f_{\mathrm{s}} a \int_{t_0}^{t} f_{\mathrm{d}} \|\boldsymbol{\varepsilon}_t(s)\| \mathrm{d}s - f_{\mathrm{s}} a^2 \Big(\mathrm{tr}(\boldsymbol{\varepsilon}(t)) - \mathrm{tr}(\boldsymbol{\varepsilon}(t_0))\Big)\right).$$

*Besides*, *the stress trace is given by*

$$\begin{aligned} \mathrm{tr}(\boldsymbol{\sigma}(t)) = \mathrm{tr}(\boldsymbol{\sigma}(t_0)) \exp\left(f_{\mathrm{s}}\Big(a^2 + \frac{1}{3}\Big)\Big(\mathrm{tr}(\boldsymbol{\varepsilon}(t)) - \mathrm{tr}(\boldsymbol{\varepsilon}(t_0))\Big)\right) \\ \times \exp\left(f_{\mathrm{s}} \int_{t_0}^{t} \Big(a f_{\mathrm{d}} \|\boldsymbol{\varepsilon}_t\| + (c_{11}\varepsilon_{11t} + 2c_{13}\varepsilon_{13t} + c_{33}\varepsilon_{33t})\mathrm{E}(\boldsymbol{\varepsilon})\Big)(s)\mathrm{d}s\right). \end{aligned} \tag{15}$$

***Proof*** Since $\varepsilon_{ijt} = 0$ in the tensor (6) for the indices $ij = 12, 21, 23, 32$, the linear equation (12a) becomes:

$$\hat{\sigma}^{\star}_{ijt} = f_{\mathrm{s}} a\Big(f_{\mathrm{d}} \|\boldsymbol{\varepsilon}_t\| - a\mathrm{tr}(\boldsymbol{\varepsilon}_t)\Big)\hat{\sigma}^{\star}_{ij}.$$

Using the separation of variable method and the following identity

$$\int_{t_0}^{t} \mathrm{tr}(\boldsymbol{\varepsilon}_t(s))\mathrm{d}s = \mathrm{tr}(\boldsymbol{\varepsilon}(t)) - \mathrm{tr}(\boldsymbol{\varepsilon}(t_0)),$$

we may easily deduce (14a). On the other hand, we note that (12a) reads

$$\hat{\sigma}^{\star}_{31t} = \hat{\sigma}^{\star}_{13t} = f_{\mathrm{s}} a\Big(a\varepsilon_{13t} + \Big(f_{\mathrm{d}} \|\boldsymbol{\varepsilon}_t\| - a\mathrm{tr}(\boldsymbol{\varepsilon}_t)\Big)\hat{\sigma}^{\star}_{13}\Big) \tag{16}$$

for $ij = 13, 31$. Hence, we solve (16) by using the variation of constants method, we find

$$\hat{\sigma}^{\star}_{13} = c_{13}\mathrm{E}(\boldsymbol{\varepsilon}) \quad \text{and} \quad c_{13t}\mathrm{E}(\boldsymbol{\varepsilon}) = f_{\mathrm{s}} a^2 \varepsilon_{13t},$$

which implies the formula (14b). In order to obtain the elements of the diagonal of $\hat{\boldsymbol{\sigma}}^{\star}$, we consider the following equations resulting from (12a):

$$\begin{aligned} \hat{\sigma}^{\star}_{22t} &= f_{\mathrm{s}} a\left(-a\frac{\varepsilon_{11t} + \varepsilon_{33t}}{3} + \Big(f_{\mathrm{d}} \|\boldsymbol{\varepsilon}_t\| - a\mathrm{tr}(\boldsymbol{\varepsilon}_t)\Big)\hat{\sigma}^{\star}_{22}\right), \\ \hat{\sigma}^{\star}_{11t} &= f_{\mathrm{s}} a\left(a\frac{2\varepsilon_{11t} - \varepsilon_{33t}}{3} + \Big(f_{\mathrm{d}} \|\boldsymbol{\varepsilon}_t\| - a\mathrm{tr}(\boldsymbol{\varepsilon}_t)\Big)\hat{\sigma}^{\star}_{11}\right), \\ \hat{\sigma}^{\star}_{33t} &= f_{\mathrm{s}} a\left(a\frac{2\varepsilon_{33t} - \varepsilon_{11t}}{3} + \Big(f_{\mathrm{d}} \|\boldsymbol{\varepsilon}_t\| - a\mathrm{tr}(\boldsymbol{\varepsilon}_t)\Big)\hat{\sigma}^{\star}_{33}\right). \end{aligned}$$

Thus, applying again the variation of constants method, we can derive the solutions given in (14c)–(14e).

To solve equation (12b), using (14b), (14d), and (14e), we first calculate the scalar product of tensors:

$$\hat{\boldsymbol{\sigma}}^{\star} : \boldsymbol{\varepsilon}_t = \hat{\sigma}^{\star}_{11}\varepsilon_{11t} + 2\hat{\sigma}^{\star}_{13}\varepsilon_{13t} + \hat{\sigma}^{\star}_{33}\varepsilon_{33t} = \big(c_{11}\varepsilon_{11t} + 2c_{13}\varepsilon_{13t} + c_{33}\varepsilon_{33t}\big)\mathrm{E}(\boldsymbol{\varepsilon}), \tag{17}$$

and insert (17) into (12b), resulting in

$$\mathrm{tr}(\boldsymbol{\sigma}_t) = f_{\mathrm{s}}\mathrm{tr}(\boldsymbol{\sigma})\Big(\Big(a^2 + \frac{1}{3}\Big)\mathrm{tr}(\boldsymbol{\varepsilon}_t) + a f_{\mathrm{d}} \|\boldsymbol{\varepsilon}_t\| + (c_{11}\varepsilon_{11t} + 2c_{13}\varepsilon_{13t} + c_{33}\varepsilon_{33t})\mathrm{E}(\boldsymbol{\varepsilon})\Big). \tag{18}$$

Finally, solving the linear ODE (18) by separation of variables provides the solution given by formula (15), thus completing the proof.

We remark that equation (14a) can be canceled from the system by setting $\hat{\sigma}^{\star}_{ij}(t_0) = 0$ for $ij = 12, 23$, because the shear strains and initial shear stress are zero for the simplified plane strain ballast model.

## Conclusion

The main results of the paper consist in refined modeling of the interaction between elastic Timoshenko beam under moving point load and hypoplastic granular track ballast. In particular, the model implies dissipative properties of normal-shear- and longitudinal strains of the hypoplastic ballast material in contact with the rough rail interface. Further direction of mathematical research of the rail-ballast interaction toward hysteresis behavior intends a non-convex sweeping process.

**Funding** Open access funding provided by University of Graz. The authors are supported by the Danube project MULT 06/2023 (Austria's Agency for Education and Internationalisation), 8X23001 (Czech Ministry of Education, Youth and Sports) and n$$^{\text {o}}$$49916UM (France Ministry for Europe and Foreign Affairs) for Austrian, Czech and French teams, respectively.

**Data availability** This manuscript has no data from repository.

## Declarations

**Conflict of interest** The authors declare no competing interests.



## REFERENCES

1. Andrews, K.T., Shillor, M., Wright, S.: On the dynamic vibrations of an elastic beam in frictional contact with a rigid obstacle. J. Elasticity. **42**(2), 1–30 (1996) https://doi.org/10.1007/BF00041221
2. Dumont, Y., Paoli, L.: Vibrations of a beam between obstacles. Convergence of a fully discretized approximation. M2AN Math. Model. Numer. Anal. **40**(4), 705–734 (2006) https://doi.org/10.1051/m2an:2006031
3. Dumont, Y., Paoli, L.: Dynamic contact of a beam against rigid obstacles: Convergence of a velocity-based approximation and numerical results. Nonlinear Anal. Real World Appl. **22**, 520–536 (2015) https://doi.org/10.1016/j.nonrwa.2014.09.009
4. Heibig, A., Petrov, A.: A dynamic Euler–Bernoulli beam equation frictionally damped on an elastic foundation. Nonlinear Anal. Real World Appl. **64**, 103427 (2022) https://doi.org/10.1016/j.nonrwa.2021.103427
5. Heibig, A., Krejčí, P., Petrov, A.: Solvability for a dynamical beam problem on a frictionally damped foundation under a moving load. Discrete Continuous Dyn. Syst. Ser. B. **28**(5), 3277–3293 (2023) https://doi.org/10.3934/dcdsb.2022217
6. Riessberger, K.: Some remarks on modern track geometry maintenance. Int. J. Railway Res. **5**(2), 9–17 (2018) https://doi.org/10.22068/IJRARE.5.2.9
7. Deiros, I., Voivret, C., Combe, G., Emeriault, F.: Ballast wear: Insight from the discrete element simulation of tracks and micro-deval tests. In: Pombo, J. (ed.) Proc. 3rd Int. Conf. on Railway Technology: Research, Development and Maintenance. Civil-Comp Press, Stirlingshire, UK (2016). Chap. 2. https://doi.org/10.4203/ccp.110.20
8. Elishakoff, I.: Handbook on Timoshenko–Ehrenfest Beam and Uflyand–Mindlin Plate Theories. World Scientific, Singapore (2020). https://doi.org/10.1142/10890
9. Rosinger, H.E., Ritchie, I.G.: On Timoshenko's correction for shear in vibrating isotropic beams. J. Phys. D: Appl. Phys. **10**(11), 1461–1466 (1977) https://doi.org/10.1088/0022-3727/10/11/009
10. Timoshenko, S.: Vibration Problems in Engineering. D. Van Nostrand Co., New York (1937)
11. Vekua, I.N.: Shell Theory, General Methods of Construction. Pitman Advanced Pub. Program, Boston, London, Melbourne (1985). https://doi.org/10.1137/10310
12. Itou, H., Khludnev, A.M.: On delaminated thin Timoshenko inclusions inside elastic bodies. Math. Methods Appl. Sci. **39**(17), 4980–4993 (2016) https://doi.org/10.1002/mma.3279
13. Khludnev, A.M., Leugering, G.: On Timoshenko thin elastic inclusions inside elastic bodies. Math. Mech. Solids. **20**(5), 495–511 (2015) https://doi.org/10.1177/1081286513505106
14. Rudoy, E.M., Lazarev, N.P.: Domain decomposition technique for a model of an elastic body reinforced by a Timoshenko's beam. J. Comput. Appl. Math. **334**, 18–26 (2018) https://doi.org/10.1016/j.cam.2017.11.019
15. Bauer, E.: Modelling limit states within the framework of hypoplasticity. AIP Conf. Proc. **1227**, 290–305 (2010) https://doi.org/10.1063/1.3435399
16. Bode, M., Mašín, D., Medicus, G., Ostermann, A.: An intergranular strain concept for material models formulated as rate equations. Int. J. Numer. Anal. Methods Geomech. **44**(7), 1003–1018 (2020) https://doi.org/10.1002/nag.3043

17. Kolymbas, D.: A Primer on Theoretical Soil Mechanics. Cambridge Univ. Press, UK (2022). https://doi.org/10.1017/9781009210348
18. Bauer, E.: Calibration of a comprehensive hypoplastic model for granular materials. Soils Found. **36**(1), 13–26 (1996) https://doi.org/10.3208/sandf.36.13
19. Gudehus, G.: A comprehensive constitutive equation for granular materials. Soils Found. **36**(1), 1–12 (1996) https://doi.org/10.3208/sandf.36.1
20. Bauer, E., Kovtunenko, V.A., Krejčí, P., Krenn, N., Siváková, L., Zubkova, A.V.: On proportional deformation paths in hypoplasticity. Acta Mechanica. **231**(4), 1603–1619 (2020) https://doi.org/10.1007/s00707-019-02597-3
21. Kovtunenko, V.A., Bauer, E., Eliaš, J., Krejčí, P., Monteiro, G.A., (Siváková), L.S.: Cyclic behavior of simple models in hypoplasticity and plasticity with nonlinear kinematic hardening. J. Sib. Fed. Univ. - Math. Phys. **14**(6), 756–767 (2021) https://doi.org/10.17516/1997-1397-2021-14-6-1-12
22. Bauer, E., Kovtunenko, V.A., Krejčí, P., Monteiro, G.A., Runcziková, J.: Stress-controlled ratchetting in hypoplasticity: a study of periodically proportional loading cycles. Acta Mechanica. **234**(9), 4077–4093 (2023) https://doi.org/10.1007/s00707-023-03596-1
23. Bauer, E., Fu, Z., Liu, S.: Influence of pressure and density on the rheological properties of rockfills. Front Struct Civ. Eng. **6**(1), 25–34 (2012) https://doi.org/10.1007/s11709-012-0143-0